

Superluminal Photonic Tunneling in Inhomogeneous Waveguides

By Klaus W. Kark¹

Abstract – Maxwell’s electrodynamics permits phase and group velocity to become superluminal (faster than the vacuum speed of light c_0) without violating Einstein causality. Both velocities fail to explain the behavior of the energy transport over evanescent modes. Apparently superluminal results follow from the use of non-causal velocity definitions such as the comparison of the peaks of the incident and the transmitted wave. However, the motion of electromagnetic waves (either propagating or tunneling) is inherently a causal and Lorentz invariant process. No signal, energy or information can travel faster than c_0 .

Index Terms – Dispersive waveguides, group velocity, delay times, Einstein causality, evanescent modes, superluminal tunneling, cutoff barrier, pulse reshaping, information transfer.

1. Introduction

Some recent publications [7,23,38] have shown up the possibility of electromagnetic waves moving with superluminal velocities higher than the vacuum speed of light c_0 . The group velocity, which is the velocity of the peak of a narrowband wave packet, has been found to become superluminal [24] in the case of evanescent modes tunneling through a cutoff barrier (**Fig. 1**). For broadband signals in dispersive transmission lines the frequency dependent group velocity should better be replaced by the peak velocity, which we will define later. However, the peaks of an incident and a transmitted (or reflected) wave packet have no causal relationship [32] and also the peak velocity may become superluminal. This does not at all mean that information can also be transmitted with superluminal speed. Since Sommerfeld and Brillouin [37] it has been known for a long time that no signal, energy or information can travel faster than c_0 .

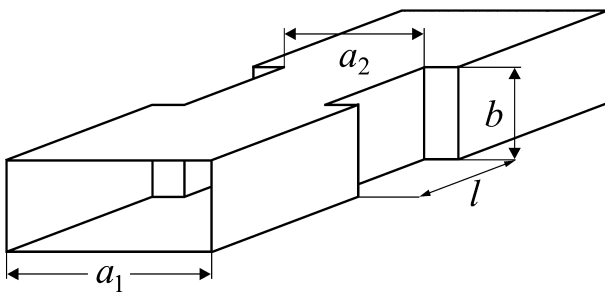


Fig. 1: Air-filled rectangular waveguide with reduced cross section. The undersized segment with length l acts as a photonic barrier for frequencies $f < c_0/(2a_2)$.

Not every mathematical quantity, which can be measured in m/s, is always and in any case a physically meaningful velocity. Actually, the main problem with superluminality seems to be the widespread unlucky use of non-causal velocity definitions and their obvious inability to describe the tunneling of evanescent modes through a cutoff barrier [6]. A pulse peak at superluminal motion does neither contradict Einstein causality nor Lorentz invariance [15]. It is just a consequence of a dispersive reshaping of the pulse form and therefore merely a simple distortion effect [14].

It is pointless to argue about superluminality with no clear definitions of signal or information in mind. Some transmission velocities (such as front, signal and energy velocity) can unambiguously be defined [4,40], so that they never exceed c_0 . Other definitions may occasionally be useful as long as they do not predict

superluminal velocities, otherwise they fail and their failure may encourage to erroneous conclusions.

This contribution gives a summary of some common definitions of velocities and delay times and discusses their causal or non-causal properties. We treat the paradox of tunneling, the analogy between the electromagnetic Helmholtz equation and the quantum mechanical Schrödinger equation (including a brief look at EPR-like composite quantum systems in entangled state) and possible misinterpretations. Detailed numerical examples consider some properties of lossy dispersive transmission lines as well as the photonic tunneling of a wave packet through cutoff barriers in rectangular waveguides.

2. Dispersion, velocities and delay times

Only the vacuum of free space is nondispersive, while all other material media or waveguides are dispersive [3]. Electromagnetic waves propagating in a dispersive medium have a phase constant $\beta(\omega) = 2\pi/\lambda(\omega)$ with *nonlinear* dependence on frequency [30]. The phenomenon of dispersion gives rise to propagation velocities changing with frequency, which is the reason why the transmission of broadband signals can lead to significant distortion effects.

2.1 Velocity definitions

Several different velocities are commonly used that were initially defined to characterize the behavior of freely propagating waves (**Tab. 1**). The **phase velocity** v_{ph} is the speed of a monochromatic wave, which extends infinitely in space and time, whereas the **group velocity** v_{gr} describes the motion of the center of gravity of a narrowband wave packet [1,30]. The **front velocity** v_F always equals the vacuum speed of light c_0 [34] and the **energy velocity** v_E that depends on the time-averaged Poynting vector \vec{S}_R and the spatial energy density w can never exceed c_0 [33,40]. Some other velocity definitions like quantile velocity, correlation velocity or centro-velocity can be found in the literature [10,12].

Tab. 1: Some common ways to define wave velocities [18].

phase velocity	$v_{ph}(\omega) = \frac{\omega}{\beta(\omega)}$
group velocity	$v_{gr}(\omega) = \frac{d\omega}{d\beta(\omega)}$
front velocity	$v_F = \lim_{\omega \rightarrow \infty} v_{ph}(\omega) = c_0 = 1/\sqrt{\mu_0 \epsilon_0}$
energy velocity	$v_E(\omega) = \frac{ \vec{S}_R }{w} = \frac{1}{2} \frac{ \text{Re}\{\vec{E} \times \vec{H}^*\} }{\frac{\epsilon}{4} \vec{E} ^2 + \frac{\mu}{4} \vec{H} ^2} \leq c_0$

¹ Hochschule für Technik, Wirtschaft und Sozialwesen Ravensburg-Weingarten, University of Applied Sciences, Weingarten, Germany

2.2 Signal transmission in dispersive media

The transmission behavior of true signals has first been studied by Sommerfeld and Brillouin [37] and [3,35,36]. In a dispersive medium – that allows waves to propagate – the rising edge of a modulated source pulse with carrier or center frequency (actually angular frequency) $\omega_0 = 2\pi f_0$ always runs with front velocity c_0 . This discontinuity is directly followed by the Sommerfeld forerunners (precursors) containing very high frequency components with very small amplitudes. If the medium contains only one electronic resonance $\omega_e > \omega_0$, the frequency of these first forerunners decreases continuously until the characteristic frequency ω_e of the oscillating electrons is reached. The second (Brillouin) forerunners follow with the reduced velocity $c = c_0/\sqrt{\epsilon_r}$ depending on the permittivity of the medium. Their frequency is at first very small, then increases constantly and finally arrives at the center frequency ω_0 of the signal. This moment marks the beginning of the main part of the transmitted signal and is related to the **signal velocity** v_s , for which the relation $v_{gr} \leq v_s \leq v_F$ must hold – provided we look at the case of freely propagating waves [3]. There is no clear mathematical definition for the signal velocity, but v_s is not far away from $v_E(\omega_0)$ (Tab. 1), if we take the energy velocity at the carrier frequency ω_0 of the source pulse. Both types of forerunners and the main signal can partly overlap depending on the length of the propagation path.

Contrary to the hitherto discussed case of freely propagating waves, a loss-free **evanescent medium** permits all higher frequency components $\omega > \omega_c$ (that lie above cutoff and build up the first forerunners) to propagate with no attenuation, while the main part of the spectrum (around $\omega_0 < \omega_c$) is evanescent and is thus exponentially suppressed according to $e^{-\alpha(\omega)z}$, since $\beta(\omega_0) = 0$ in a loss-free tunneling region. So, phase and group velocity v_{ph} and v_{gr} will become infinite (see Tab. 1) and lose their physical meaning. On the other hand, front, energy and signal velocity (v_F, v_E, v_s) are still well defined and stay applicable for evanescent modes – also useful are some delay time definitions that will be discussed below.

2.3 Delay times

Linear, time-invariant (LTI) systems can be described by a complex transfer function:

$$\underline{H}(j\omega) = H(\omega) e^{j\Phi(\omega)} = \int_{-\infty}^{\infty} h(t) e^{-j\omega t} dt. \quad (1)$$

$\underline{H}(j\omega)$ is the Fourier transform of $h(t)$, which is called impulse response and would be the system's output signal if the input signal were a Dirac impulse $\delta(t)$ located at $t = 0$. In causal systems the impulse response must vanish at negative times, i. e. $h(t) \equiv 0$ for $t < 0$. The magnitude and the phase spectra $H(\omega)$ and $\Phi(\omega)$ are real-valued even and odd continuous functions of ω , respectively. Of course, no technical source can send out photons with extremely high energies $E = \hbar\omega$. Thus, quantum effects limit the validity of the classical concept of purely continuous spectra. However, this limitation arises only at exceptionally high frequencies $\omega > E/\hbar$, which are by far of no technical interest.

Using the phase spectrum $\Phi(\omega)$, we define the **phase delay** and the **group delay** as follows [39]:

$$t_{ph}(\omega) = -\frac{\Phi(\omega)}{\omega} \quad \text{and} \quad t_{gr}(\omega) = -\frac{d\Phi(\omega)}{d\omega}. \quad (2)$$

With these delay times we get spatially averaged phase and group velocities [9] for signals traversing a distance z :

$$\overline{v_{ph}}(z, \omega) = \frac{z}{t_{ph}(\omega)} \quad \text{and} \quad \overline{v_{gr}}(z, \omega) = \frac{z}{t_{gr}(\omega)}. \quad (3)$$

Since both delay times (2) and both averaged velocities (3) depend on frequency ω , they are not well suited to describe the motion of a localized wave packet covering a certain frequency range. For such problems we better use center of gravity definitions that have more physical significance. We will derive them on basis of a *causal* LTI system shown in **Fig. 2** with $h(t) \equiv 0$ for $t < 0$. Furthermore we will always assume the input signal to vanish at negative times, i.e. $x(t) \equiv 0$ for $t < 0$.

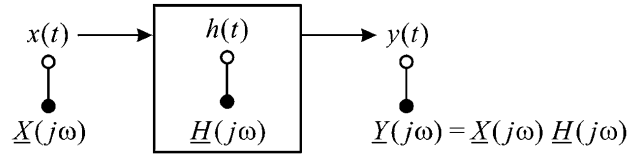


Fig. 2: Causal LTI system with input signal $x(t)$, output signal $y(t)$ and impulse response $h(t)$.

The output signal $y(t)$ is found either by convolution or by spectral domain methods [16]:

$$y(t) = x(t) * h(t) = \int_0^t x(u) h(t-u) du = \frac{1}{2\pi} \int_{-\infty}^{\infty} \underline{X}(j\omega) \underline{H}(j\omega) e^{j\omega t} d\omega. \quad (4)$$

The centers of gravity for input and output signal

$$t_x = \frac{\int_0^{\infty} t x(t) dt}{\int_0^{\infty} x(t) dt} \quad \text{and} \quad t_y = \frac{\int_0^{\infty} t y(t) dt}{\int_0^{\infty} y(t) dt} \quad (5)$$

do not coincide, but differ by the **center delay** [21]

$$t_h = \frac{\int_0^{\infty} t h(t) dt}{\int_0^{\infty} h(t) dt} = t_y - t_x = t_{gr}(\omega = 0). \quad (6)$$

It can be shown [31] that t_h is identical to the group delay (2) computed at $\omega = 0$. Therefore (6) should only be applied to unmodulated baseband signals in low pass transmission systems. For systems with high pass transfer functions – such as waveguide systems – the **impulse delay**

$$t_i = \frac{\int_0^{\infty} t h^2(t) dt}{\int_0^{\infty} h^2(t) dt} \quad (7)$$

proposed by [22] is more useful. With Parseval's relation [16] we can show that t_i can also be computed in the spectral domain:

$$t_i = \frac{\int_0^{\infty} t_{gr}(\omega) H^2(\omega) d\omega}{\int_0^{\infty} H^2(\omega) d\omega}. \quad (8)$$

Thus, t_i results from a spectral averaging of the frequency dependent group delay $t_{gr}(\omega)$ and can be considered as a **mean group delay**. It marks the **energy center** of the output signal $y(t)$ for systems, which are excited by a Dirac impulse $\delta(t)$. More general excitation functions will be discussed in the following.

2.4 Energy center and effective duration of a signal

Let us again consider the causal LTI system of Fig. 2 excited by a real input signal $x(t)$ vanishing at $t < 0$. We use the *energy* of the signal

$$E_0 = \int_0^{\infty} x^2(t) dt \quad (9)$$

together with first and second moments

$$E_1 = \int_0^{\infty} t x^2(t) dt \quad \text{and} \quad E_2 = \int_0^{\infty} t^2 x^2(t) dt \quad (10)$$

and define - according to [44] - the time position of the **energy center** τ_x and the effective (quadratic) signal duration or **time spread** d_x :

$$\tau_x = \frac{E_1}{E_0} \quad \text{and} \quad d_x = \sqrt{\frac{E_2}{E_0} - \tau_x^2} \quad (11)$$

The energy center τ_x lies in the immediate vicinity of the peak value of $x(t)$ and represents the classical particle position [44] associated with the quantum mechanical wave function ψ in (15), provided that $\hbar\omega > V(z)$. The time shift between the energy centers of the output signal $y(t)$ and the input signal $x(t)$ will be called **peak delay** t_p . It may take positive or negative values:

$$t_p = \tau_y - \tau_x = \frac{\int_0^{\infty} t y^2(t) dt}{\int_0^{\infty} y^2(t) dt} - \frac{\int_0^{\infty} t x^2(t) dt}{\int_0^{\infty} x^2(t) dt} \quad (12)$$

It is worthy of note that t_p equals t_p , if we consider the special case $x(t) = \delta(t)$, resulting in $y(t) = h(t)$. But (12) is more general than (7), since t_p can be used for all kinds of input signals (vanishing for negative times).

3. Einstein causality and evanescent modes

All signals with finite duration have an unlimited spectrum and necessarily suffer from dispersion. In loss-free media the wave number $\underline{k}(\omega) = \beta(\omega)$ is real for the propagating part of the spectrum and imaginary for the evanescent part, i.e. $\underline{k}(\omega) = -j\alpha(\omega)$. Then, a signal is partly delayed (with changing phases) and partly weakened (with constant phases), respectively. The “propagation” of evanescent modes over a distance z seems to take no time, which leads to the paradox of tunneling (see below). The resulting distortions of the pulse shape – following from frequency selective damping – can be mistaken for a loss of causality. For later convenience, we extend (12) to spatially distributed systems with length z . **Einstein causality** requires the output signal to vanish until the very first wave front has arrived with the vacuum speed of light c_0 :

$$\begin{aligned} x(t) &\equiv 0 & \text{for } t < 0 \\ y(t) &\equiv 0 & \text{for } t < z/c_0 \\ h(t) &\equiv 0 & \text{for } t < z/c_0. \end{aligned} \quad (13)$$

Thus, we get the **peak delay** for $z \geq 0$:

$$t_p(z) = \tau_y(z) - \tau_x = \frac{\int_{z/c_0}^{\infty} t y^2(t) dt}{\int_{z/c_0}^{\infty} y^2(t) dt} - \frac{\int_0^{\infty} t x^2(t) dt}{\int_0^{\infty} x^2(t) dt} \quad (14)$$

3.1 The paradox of tunneling

The front of any causal signal $y(t)$ according to (13), which has an unlimited frequency band due to Fourier transform, travels with $v_F = c_0$ (Tab. 1). On the other hand the peak of this signal may travel with superluminal velocity when crossing a photonic barrier [23]. This peak is located in the neighborhood of the energy center $\tau_y(z)$. Using the peak delay (14) we can define a spatially averaged **peak velocity** $\bar{v}_p(z) = z/t_p(z)$, quite similar as we did in (3). Every tunneling region with suitable length z can produce a value of $\bar{v}_p(z)$ that is higher than c_0 . The peak velocity, which is obviously not a genuine signal velocity, must not be confused with the energy velocity $v_E(\omega)$, defined in Tab. 1.

Although it may happen that the peak velocity is superluminal, i.e. $\bar{v}_p(z) > c_0$, the principle of Einstein causality is never violated, because of $y(t) \equiv 0$ for $t < z/c_0$. The peaks of the pulses in front and behind the evanescent barrier have no causal relationship [32]. Thus, cause and effect cannot be interchanged and back-in-time communication, which would imply a change of chronological order, is impossible. In addition, no portion of energy can travel faster than light, since $v_E(\omega) \leq c_0$ applies for all frequencies. What we really see, if the peak velocity is superluminal, is just a shift of the energy center towards the front of the signal. This distortion effect – due to the high pass filter characteristic of the evanescent region – only leads to a simple pulse reshaping and no physical conflict emerges.

Some authors argue that pulse reshaping should vanish for narrowband or band-limited signals [25,27]. But this is only true for strictly monochromatic signals (carrying no information at all) or if we look at hypothetical distortion-free communication systems (with transfer function $\underline{H}(j\omega) = Ke^{-j\omega t_0}$) that firstly cannot be realized and secondly have nothing to do with evanescent tunneling. Unimportant whether pulse reshaping occurs or not, the signal velocity is always limited by the vacuum speed of light, i. e. $v_S \leq v_F \leq c_0$.

3.2 The quantum mechanical analogy

We consider the **Schrödinger equation** for the quantum mechanical wave function ψ of a non-relativistic particle with mass m and total energy $E = \hbar\omega$ moving in a nonuniform medium with potential $V(z)$:

$$\frac{\partial^2 \psi}{\partial z^2} + \frac{2m}{\hbar^2} (\hbar\omega - V(z)) \psi = 0 \quad (15)$$

For $\hbar\omega > V(z)$ we find propagation in a dispersive medium, while $\hbar\omega < V(z)$ describes a damped wave packet tunneling through a potential barrier. Let us now compare (15) with the scalar **Helmholtz equation** for the longitudinal magnetic field component of a TE waveguide mode:

$$\frac{\partial^2 H}{\partial z^2} + \frac{1}{c^2} (\omega^2 - \omega_c^2(z)) H = 0 \quad (16)$$

The popular use of the formal analogy relating (15) and (16) – particularly the connection between tunneling particles and cutoff modes in waveguides – has led to serious confusion in the literature. The (Lorentz invariant) transmission of truly *relativistic* electromagnetic modes through a photonic barrier has been compared with the (Galilei invariant) quantum mechanical tunneling of *non-relativistic* particles through an energy band gap [24]. But this overstressed **photon-particle analogy** is obviously inappropriate [28] and may be one reason for fundamental misinterpretations.

Some really strange statements in the literature [25,26] such as – “evanescent modes have *nonlocal* properties and consequently are not fully describable by Maxwell’s equations, or evanescent modes have *negative* energy and therefore cannot be measured, or evanescent modes are *not* Lorentz invariant, or evanescent modes have a superluminal *signal* velocity and *violate* Ein-

stein causality” – are in fact totally absurd and have already been proven to be false [4,11,19,29,42].

Composite quantum systems in entangled state, which consist of two spatially separated EPR-like correlated subsystems (EPR means Einstein-Podolsky-Rosen), may have peculiar properties [41]. The measurement, carried out in one subsystem, induces *instantaneous* changes of the other [2] - no matter how large their mutual distance actually will be - why this phenomenon has also been called “spooky interaction at a distance”. The nonlocal interaction of two entangled photons can only be described by a set of *two* coupled Schrödinger equations and therefore has no comparable electromagnetic analogy at all. Even in the peculiar world of quantum mechanics such **nonlocal EPR effects** cannot be used for superluminal transmission of information [5]. There seems to be a superior principle in quantum mechanics and also in electrodynamics that prevents superluminal information or signal or energy transport.

4. Numerical examples

4.1 Homogeneous waveguide with lossy walls

Before covering inhomogeneous waveguide structures, we will discuss a dispersing wave packet (in form of a TE₁₀ mode with cutoff frequency $\omega_c = c_0 \pi/a$), traveling in positive z-direction through a homogeneous air-filled rectangular waveguide with finite wall conductivity κ (Fig. 3).

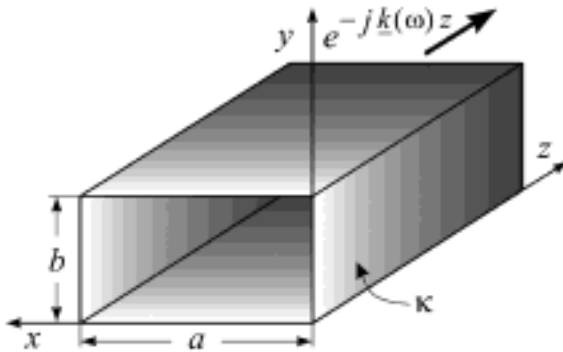


Fig. 3: Homogeneous air-filled rectangular waveguide – with ohmic losses due to wall currents.

First of all, a **sharp cutoff** exists only in loss-free waveguides [43,45]. Then, the low-frequency part of the spectrum ($\omega \leq \omega_c$) is purely evanescent, while all frequencies above cutoff ($\omega > \omega_c$) are purely propagating. This situation can be described by a complex wave number:

$$\underline{k}(\omega) = \begin{cases} \beta(\omega) = \sqrt{\omega^2 - \omega_c^2}/c_0 & \text{for } \omega > \omega_c \\ -j\alpha(\omega) = -j\sqrt{\omega_c^2 - \omega^2}/c_0 & \text{for } \omega \leq \omega_c \end{cases} \quad (17)$$

On the other hand, a realistic waveguide with ohmic losses due to finite wall conductivity κ has no sharp cutoff, but rather a **gradual transition** between evanescent and propagating state. For good wall conductivity $\kappa \gg \omega \epsilon_0$ there is also a small phase constant β below ω_c and a small attenuation constant α above ω_c . Mainly in the vicinity of ω_c Eq. (17) is no longer valid and a more sophisticated treatment is needed, which takes the coupling between TE and TM modes into account. Thus, we finally arrive at a better approximation of the **complex wave number** for a TE₁₀ mode in rectangular waveguides with lossy walls [8], applicable for all frequencies ω :

$$\underline{k}(\omega) = \beta(\omega) - j\alpha(\omega) = \frac{1}{c_0} \sqrt{\omega^2 - \omega_c^2 + (1-j)\delta \left(\frac{\omega^2}{b} + \frac{2\omega_c^2}{a} \right)} \quad (18)$$

Both constants α and β must be positive and $\delta = \sqrt{2/(\omega \mu_0 \kappa)}$ is the skin depth of the metallic walls. Eq. (18) cannot be found by ordinary power-loss methods, but is the result of a more complicated Ritz technique in connection with variational principles [8]. We solve (18) for α and β in the case of a standard R100 aluminum waveguide ($a = 22,86$ mm, $b = 10,16$ mm and $\kappa = 36 \cdot 10^6$ S/m). In particular, we get $\alpha(\omega_c) \approx 0,868$ and $\beta(\omega_c) \approx 2,095$, which is in contrast with the result $\alpha(\omega_c) = \beta(\omega_c) = 0$ of the more simple theory (17). Using the attenuation per unit length $d = 20 \lg e^\alpha$ dB/m = $8,686 \alpha$ dB/m, the frequency dependence of d and β is shown in Fig. 4.

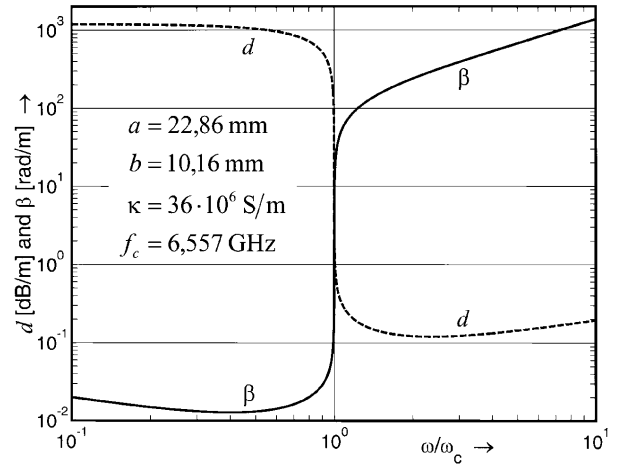


Fig. 4: Attenuation per unit length d and phase shift per unit length β for a TE₁₀ mode in a R100 rectangular aluminum waveguide.

With the phase constant $\beta(\omega)$ from Fig. 4 we can easily compute the **phase velocity** $v_{ph} = \omega/\beta$ and the **group velocity** $v_{gr} = d\omega/d\beta$. Both results are shown in Fig. 5. Above cutoff ($\omega > \omega_c$), the well-known **Born relation** $v_{ph} v_{gr} = c_0^2$ is met. Below cutoff ($\omega < \omega_c$), both velocities may become superluminal.

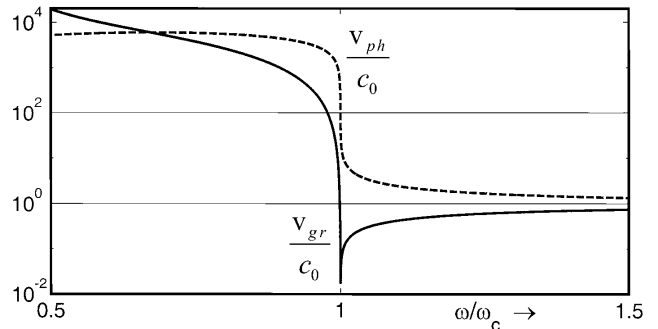


Fig. 5: Phase and group velocity of a TE₁₀ mode in a R100 rectangular aluminum waveguide.

Let us now consider an **input signal** $x(t)$ with rectangular envelope of normalized amplitude 1, carrier frequency $f_0 = 10$ GHz and duration 1 ns, with $\tau_x = 0,5$ ns according to (11), fed in a standard R100 aluminum lossy waveguide ($a = 22,86$ mm, $b = 10,16$ mm and $\kappa = 36 \cdot 10^6$ S/m) at position $z = 0$. The causal **output signal** $y(t)$ after a distance $z \geq 0$ follows from (4) and (13):

$$\begin{aligned} y(t) &= \int_{u=0}^{t-z/c_0} x(u) h(t-u) du = \\ &= \frac{1}{2\pi} \int_{u=0}^{t-z/c_0} x(u) \int_{\omega=-\infty}^{\infty} e^{j[\omega(t-u) - \underline{k}(\omega)z]} d\omega du, \end{aligned} \quad (19)$$

using a high pass transfer function $\underline{H}(j\omega) = e^{-jk(\omega)z}$ (see Fig. 6) with $\underline{k}(\omega)$ according to (18).

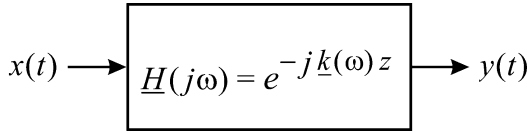


Fig. 6: Dispersive high pass waveguide system with causal output signal $y(t)$ at position $z \geq 0$.

With (19) we get the output signal $y(t)$ at a distance $z = 10$ m, shown in Fig. 7, which has been determined with a computer code adapted from [17].

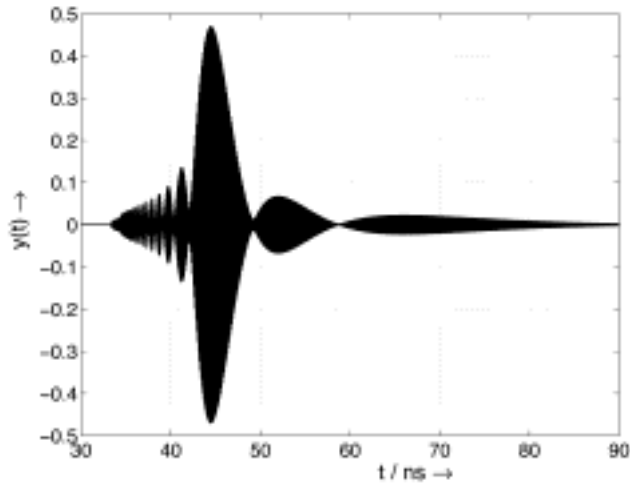


Fig. 7: Output signal $y(t)$ at position $z = 10$ m in a R100 rectangular aluminum waveguide resulting from an input TE_{10} signal $x(t)$ at $z = 0$ with rectangular envelope of normalized amplitude 1, duration 1 ns and carrier frequency 10 GHz (high above the cutoff frequency 6,557 GHz).

The first forerunners – with very high frequency components at low amplitudes – arrive at $t = z/c_0 \approx 33,36$ ns. Using (14) we get the **energy center** $\tau_y(z = 10 \text{ m}) = 45,51$ ns, which is located in the main part of the signal – a short time after the pulse peak. With $\tau_x = 0,5$ ns and the peak delay $t_p(z) = \tau_y(z) - \tau_x \approx 44,65$ ns we get the spatially averaged **peak velocity** of the energy center:

$$\bar{v}_p(z) = \frac{z}{t_p(z)} \approx 0,747 c_0, \quad (20)$$

which is comparable with the TE_{10} **group velocity**, computed at carrier frequency $f_0 = 10$ GHz:

$$v_{gr}(\omega_0) = c_0 \sqrt{1 - (\omega_c/\omega_0)^2} \approx 0,755 c_0. \quad (21)$$

Essentially, Fig. 7 shows that $y(t)$ is widely spread and dispersed. Its effective (quadratic) duration or **time spread** follows from (11):

$$d_y(z) = \sqrt{\frac{\int_{z/c_0}^{\infty} t^2 y^2(t) dt}{\int_{z/c_0}^{\infty} y^2(t) dt} - \tau_y^2(z)} \approx 4,85 \text{ ns} \quad (\text{at } z = 10 \text{ m}). \quad (22)$$

A detailed investigation of R100 waveguides with various lengths, but always excited by the same input signal $x(t)$, leads to an *asymptotic* approximation of the time spread (with $d_0 = 0,288$ ns) that is accurate to $< 4,4\%$ for all $z > 2,3$ m:

$$d_y(z) \approx \sqrt{d_0^2 + z(z + 85,2 \text{ m}) / (21,9 c_0)^2}. \quad (23)$$

Thus, the effective duration of a wave packet is increasing with distance z . Its **mean attenuation** $\bar{\alpha}$ can be found by comparison between input and output energy:

$$e^{2\bar{\alpha}z} = \frac{\int_0^{\infty} x^2(t) dt}{\int_{z/c_0}^{\infty} y^2(t) dt} \approx 1,41 \hat{=} 1,5 \text{ dB} \xrightarrow{z=10 \text{ m}} \bar{\alpha} \approx 0,017 \text{ m}^{-1}, \quad (24)$$

which is very similar to the attenuation at the carrier frequency $\alpha(\omega_0) \approx 0,016 \text{ m}^{-1}$ that can directly be found using (18). We should mention that the **attenuation of the main peak value** is much higher, namely $20 \lg(1/0,47) \approx 6,56$ dB (see Fig. 7), which is a consequence of the large number of minor peaks in $y(t)$.

4.2 Dielectrically loaded waveguides

As we already stated for homogeneous waveguides, the phase and the group velocity may easily become higher than c_0 (Fig. 5). Hence, superluminal values of v_{ph} and v_{gr} are in no way useful to describe the transport of energy or information. Once again, we will demonstrate this with a *loss-free* rectangular R100 waveguide that consists of three homogeneous sections. Sections (1) and (3) are filled with a *loss-free* dielectric material ($\epsilon_r = 2,56$) and section (2) is an air gap of length $l = 5$ cm (Fig. 8). The waveguide is excited at $z = -100$ cm by an **input signal** $x(t)$ with cosine squared envelope of normalized amplitude 1, carrier frequency $f_0 = 6$ GHz and duration 4 ns. Thus, $x(t)$ consists of 24 temporal periods and has its energy center $\tau_x = 2$ ns exactly in the middle. The carrier frequency f_0 was chosen to fulfill the condition $f_{c,1} < f_0 < f_{c,2}$ with the cutoff frequencies of the air section $f_{c,2} = 6,557$ GHz and the dielectric section $f_{c,1} = f_{c,2} / \sqrt{\epsilon_r} = 4,098$ GHz.

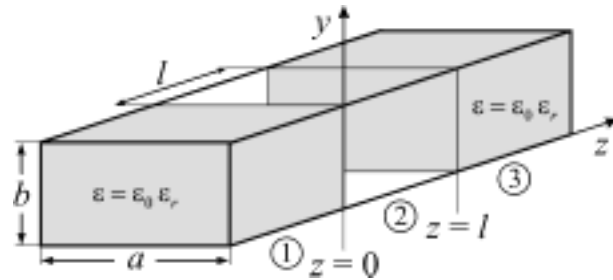


Fig. 8: Dielectrically loaded rectangular waveguide with an air gap (tunnel) of length $l = 5$ cm

The exact solution must satisfy the boundary conditions at $z = 0$ and $z = l$, respectively and can be found in [18,19]. The **spatial movement** of a cosine squared wave packet is shown in Fig. 9 using discrete time steps $\Delta t = 454,5$ ps.

With the phase velocity in the dielectrically loaded sections (1) and (3) we get the **guide wavelength** at carrier frequency:

$$\lambda_1(\omega_0) = \frac{2\pi v_{ph,1}(\omega_0)}{\omega_0} = \frac{2\pi c_0 / \sqrt{\epsilon_r}}{\sqrt{\omega_0^2 - \omega_{c,1}^2}} \approx 4,276 \text{ cm}. \quad (25)$$

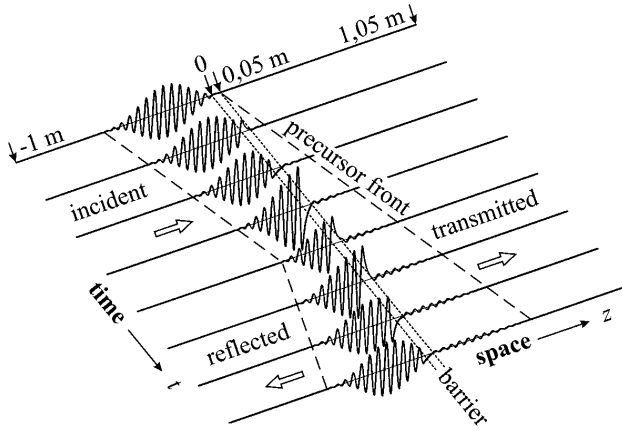


Fig. 9: Spatial distribution of a cosine squared wave packet $y(z)$ incident at a cutoff barrier of length $l = 5$ cm.

While the **Brillouin precursors** propagate with velocity $c = c_0/\sqrt{\epsilon_r}$, they move about $c\Delta t \approx 8,517$ cm $\approx 1,992 \lambda_1$ per each time step. We call attention to the fact that 24 temporal periods in $x(t)$ only lead to nearly 17,5 spatial periods in $y(z)$. This reduction is due to the difference between phase velocity (25) and precursor velocity:

$$\frac{v_{ph,1}(\omega_0)}{c_0/\sqrt{\epsilon_r}} = \frac{\lambda_1(\omega_0)}{\lambda_0/\sqrt{\epsilon_r}} = \frac{1}{\sqrt{1 - (\omega_{c,1}/\omega_0)^2}} \approx 1,37. \quad (26)$$

Especially, we are interested in the **time dependence** of the signals $y(t, z = 0)$ at the beginning and $y(t, z = l)$ at the end of the cutoff barrier. After tunneling through the air gap the output signal is considerably weakened and has been enlarged twenty times for graphical reasons (Fig. 10).

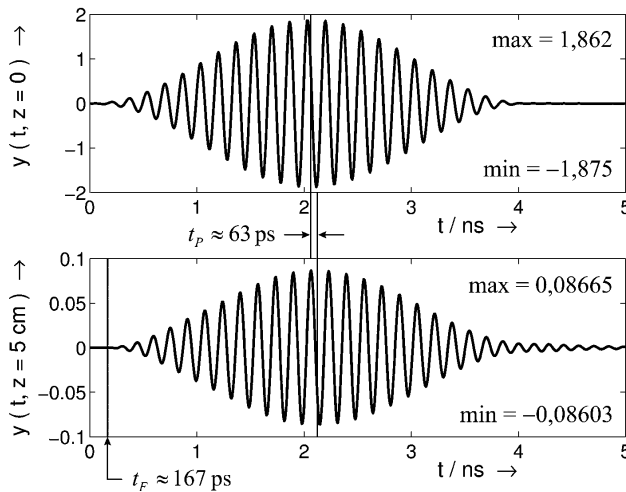


Fig. 10: Time signals $y(t)$ at $z = 0$ and behind the air gap at $z = l = 5$ cm (see Fig. 8).

For $y(t, z = 0)$ we get a peak value of almost 2, since there is a superposition of incident and reflected waves. The energy centers and the time spreads for the signal $y(t, z = 0)$ just in front of the barrier and for the signal $y(t, z = 5$ cm) directly behind the barrier are shown in **Tab. 2**.

Tab. 2: Position of energy centers and time spreads for the signals of Fig. 10.

	$y(t, z = 0)$	$y(t, z = 5$ cm)
energy center	$\tau_y = 2,061$ ns	$\tau_y = 2,124$ ns
time spread	$d_y = 0,569$ ns	$d_y = 0,585$ ns

The peak delay

$$t_p(l) = \tau_y(z = l = 5$$
 cm) $- \tau_y(z = 0) \approx 63$ ps (27)

is sometimes understood as **tunneling time** or dwell time of the evanescent wave packet in the air gap. However, in order to avoid misinterpretations, the peak delay should be better considered as a measure for distortions of the pulse shape [14]. It is worth mentioning that $t_p(l)$ significantly depends on the tunnel length l . Using (20) and (27) we get the spatially averaged **peak velocity** of the energy center, when crossing a tunnel of length $l = 5$ cm:

$$\bar{v}_p(l) = \frac{l}{t_p(l)} \approx 2,65 c_0. \quad (28)$$

The peak velocity is **superluminal**, no doubt about it. However, the peaks of the wave packets in front and behind an evanescent barrier are not causally related. While tunneling, there merely happens a shift of the energy center towards the front of the signal. This distortion effect only leads to a simple reshaping of the pulse envelope. The very first front of $y(t, z = 5$ cm) arrives at $t_F = l/c_0 \approx 167$ ps (see Fig. 10). Hence, causal propagation at exactly the vacuum speed of light c_0 is guaranteed, even for evanescent modes in cutoff barriers.

As well as the peak velocity $\bar{v}_p(l)$, also the phase velocity $\bar{v}_{ph}(l, \omega)$ and the group velocity $\bar{v}_{gr}(l, \omega)$ can become superluminal when crossing the barrier. To demonstrate this, we consider the phase difference $\Phi(\omega)$ between the transmitted wave at $z = l = 5$ cm and the incident wave at $z = 0$. For frequencies in the evanescent range $\omega_{c,1} < \omega < \omega_{c,2}$ with $\omega_{c,2} = c_0\pi/a$ and $\omega_{c,1} = \omega_{c,2}/\sqrt{\epsilon_r}$ we use the expression given in [18]:

$$\Phi(\omega) = \frac{\pi}{2} - \arctan\left(\frac{2\alpha_2\beta_1}{\alpha_2^2 - \beta_1^2} \coth(\alpha_2 l)\right) \quad (29)$$

with the phase and attenuation constants of the waveguide sections (1) and (2):

$$\beta_1 = \sqrt{\epsilon_r \omega^2 - \omega_{c,2}^2}/c_0$$

$$\alpha_2 = \sqrt{\omega_{c,2}^2 - \omega^2}/c_0. \quad (30)$$

For sufficiently large damping, e.g. $\alpha_2 l \geq 2$, the phase function (29) will become *independent* of the barrier length l , since $\coth(\alpha_2 l) \rightarrow 1$. Under this assumption, we insert (30) in (29) and derive

$$\Phi(\omega) \approx \frac{\pi}{2} - 2 \arctan \frac{\sqrt{\epsilon_r - (\omega_{c,2}/\omega)^2}}{\sqrt{(\omega_{c,2}/\omega)^2 - 1}}. \quad (31)$$

Differentiating (31) with respect to ω yields the **group delay** (2), valid for $1/\sqrt{\epsilon_r} < \omega/\omega_{c,2} < 1$:

$$t_{gr}(\omega) \approx \frac{1}{\pi f} \frac{1}{\sqrt{\epsilon_r (\omega/\omega_{c,2})^2 - 1}} \frac{1}{\sqrt{1 - (\omega/\omega_{c,2})^2}} \quad (32)$$

At carrier frequency $f_0 = 6$ GHz we find a group delay $t_{gr}(\omega_0) \approx 123$ ps, which is truly independent of the barrier length l (if $\alpha_2 l \geq 2$) and can consequently only result from localized phase shifts at the barrier boundaries. The same effect of **universal tunneling time** (also with reference to group delay) has been proven for quantum mechanical tunneling as well [13]. For that reason, some authors [25] have argued that tunneling itself takes no time. However, the group delay $t_{gr}(\omega)$ and also the peak delay $t_p(l)$ are inappropriate measures for evanescent modes. A correct description should rather use the front delay $t_f(l) = l/c_0$, which always increases with barrier length and defines the genuine propagation time. So, tunneling is not at all instantaneous but definitely time consuming.

Using (2), (3), (31) and (32) we finally get the expected superluminal values (at the carrier frequency $f_0 = 6$ GHz with $\alpha_2 l \approx 2,77$) for **phase velocity** and **group velocity**:

$$\overline{v_{ph}(l, \omega_0)} = \frac{-l}{\Phi(\omega_0)/\omega_0} \approx 7,4 c_0 \quad (33)$$

$$\overline{v_{gr}(l, \omega_0)} = \frac{l}{t_{gr}(\omega_0)} \approx 1,4 c_0$$

The superluminal results (33) are not really surprising, because already Sommerfeld knew about possible problems arising in connection with the definitions of phase and group velocity. He considered the reactive near field ($r < \lambda_0/2$) of a Hertzian dipole in free space with stationary harmonic excitation and also found superluminal values of $\overline{v_{ph}}$ and $\overline{v_{gr}}$, which even tend towards infinity [20] for $r \rightarrow 0$.

5. Conclusions

To summarize, the phase, group and peak velocity are by no means physically valuable quantities to describe the energy, signal or information transfer through cutoff barriers. The use of these definitions should be restricted only to propagating waves. They totally fail to explain the behavior of the energy transport over evanescent modes and may lead to the erroneous conclusion of propagation faster than c_0 . The tunneling of evanescent modes can completely be described within the classical framework of Maxwell's equations and leaves no choice for further-reaching interpretations. Exactly one century after its discovery by Einstein, the special theory of relativity has once again shown its unconditional validity. As a rigorous result, the front velocity v_f sets an upper bound for the speed of information transfer. Consequently, superluminal signaling turns out to be an illusion.

Acknowledgements

I want to express my gratitude to Professor Dr. B. Schnizer from the Institute of Theoretical and Computational Physics of Graz University of Technology (Austria) for his encouragement to write this article, for helpful discussions and for his support in retrieving useful publications.

References

- [1] Born, M.; Wolf, E.: Principles of optics. Cambridge, University Press, 1997.
- [2] Bouwmeester, D.; Pan, J.-W.; Mattle, K.; Eibl, M.; Weinfurter, H.; Zeilinger, A.: Experimental quantum teleportation. Nature 390 (1997), 575–579.
- [3] Brillouin, L.: Wave propagation and group velocity. New York, Academic Press, 1960.
- [4] Brunner, N.; Scarani, V.; Wegmüller, M.; Legré, M.; Gisin, N.: Direct measurement of superluminal group velocity and signal velocity in an optical fiber. Physical Review Letters 93 (2004), 203902.
- [5] Bruß, D.; D'Ariano, G. M.; Macchiavello, C.; Sacchi, M. F.: Approximate quantum cloning and the impossibility of superluminal information transfer. Phys. Rev. A 62 (2000), 062302.
- [6] Büttiker, M.; Thomas, H.: Front propagation in evanescent media. Annalen der Physik (Leipzig) 7 (1998), 602–617.
- [7] Chiao, R. Y.; Kwiat, P. G.; Steinberg, A.M.: Schneller als das Licht? Spektrum der Wissenschaft (1993), 40–49.
- [8] Collin, R. E.: Field theory of guided waves. New York, IEEE Press, 1991.
- [9] Czyliwki, A.: On the velocity of information transmitted via systems with high-pass character. Int. J. Electron. Commun. (AEÜ) 53 (1999), 121–128.
- [10] Dahmen, H. D.; Gjonaj, E.: Wellenprozesse und Kausalität: Eine Untersuchung von elektromagnetischen Signalen in Hohlleitern variablen Querschnitts. Workshop on Superluminal Velocities, Cologne University, 1998.
- [11] Ghose, P.; Samal, M. K.: Lorentz-invariant superluminal tunneling. Physical Review E, 64 (2001), 036620.
- [12] Goenner, H.: Einstein causality and the superluminal velocities of the Cologne microwave experiment. Ann. Phys. (Leipzig) 7 (1998), 774–782.
- [13] Hartman, T. E.: Tunneling of a wave packet. Journal of Applied Physics 33 (1962), 3427–3433.
- [14] Hoffmann, M. H. W.: Hochfrequenztechnik. Berlin, Springer, 1997.
- [15] Jackson, J. D.: Klassische Elektrodynamik. Berlin, de Gruyter, 1983.
- [16] Jackson, L. B.: Signals, systems and transforms. Reading (MA), Addison-Wesley, 1991.
- [17] Jäger, H. R.: Analyse der Ausbreitung von Impulsen in Mikrowellenschaltungen. Diploma Thesis, University of Applied Sciences Ravensburg-Weingarten, 1998.
- [18] Kark, K. W.: Wie schnell ist schnell? Geschwindigkeitsdefinitionen bei der Übertragung von Signalen. Frequenz 53 (1999), 226–232.
- [19] Kark, K. W.: Zum Tunneleffekt in Cutoff-Bereichen von Hohlleitern. Kleinheubacher Berichte 43 (2000), 411–419.
- [20] Kark, K. W.: Antennen und Strahlungsfelder - Elektromagnetische Wellen auf Leitungen, im Freiraum und ihre Abstrahlung. Wiesbaden, Vieweg, 2004.
- [21] Marko, H.: Korrelation und Vorausbestimmung von Signalen. VDE Fachberichte 19 (1956).
- [22] Morgenstern, G.: Gruppenlaufzeit und Impulslaufzeit. Int. J. Electron. Commun. (AEÜ) 25 (1971), 393–395.
- [23] Nimtz, G.: Instantanes Tunneln – Tunnelexperimente mit elektromagnetischen Wellen. Phys. Bl. 49 (1993), 1119–1120.
- [24] Nimtz, G.: Schneller als das Licht? Physik in unserer Zeit 28 (1997), 214–218.
- [25] Nimtz, G.; Heitmann, W.: Superluminal photonic tunneling and quantum electronics. Prog. Quant. Electr. 21 (1997), 81–108.
- [26] Nimtz, G.: Superluminal signal velocity. Annalen der Physik (Leipzig) 7 (1998), 618–624.
- [27] Nimtz, G.: On superluminal tunneling. Prog. Quant. Electr. 27 (2003), 417–450.
- [28] Nitsch, J.: Werden Signale durch Tunnelstrecken wirklich mit Überlichtgeschwindigkeit übertragen? Magdeburger Wissenschaftsjournal 4 (1999), 11–19.
- [29] Omar, A.S.; Kamel, A.H.: Network theoretical transient analysis of signal transmission over evanescent modes. IEEE Trans. Ant. Prop. AP-51 (2003), 595–605.
- [30] Piefke, G.: Feldtheorie. Band I, II und III. Mannheim, Bibliographisches Institut, 1977.
- [31] Rupprecht, W.: Lineare Netzwerke mit negativer Gruppenlaufzeit. PhD Thesis, Karlsruhe University, 1961.
- [32] Sauter, T.: Superluminal signals: an engineer's perspective. Physics Letters A 282 (2001), 145–151.
- [33] Schumann, W.O.: Elektrische Wellen. München, Hanser, 1948.
- [34] Sexl, R.; Urbantke, H.K.: Relativität, Gruppen, Teilchen. Wien, Springer, 1982.
- [35] Sommerfeld, A.: Vorlesungen über Theoretische Physik, Band II: Mechanik der deformierbaren Medien. Thun, Harri Deutsch, 1992.
- [36] Sommerfeld, A.: Vorlesungen über Theoretische Physik, Band IV: Optik. Thun, Harri Deutsch, 1978.
- [37] Sommerfeld, A.; Brillouin, L.: Über die Fortpflanzung des Lichtes in dispergierenden Medien. Annalen der Physik 44 (1914), 177–240.
- [38] Steinberg, A.M.; Myrskog, S.; Moon, H.S.; Kim, H.A.; Fox, J.; Kim, J. B.: An atom optics experiment to investigate faster-than-light tunneling. Ann. Phys. (Leipzig) 7 (1998), 593–601.

[39] Steinbuch, K.; Rupprecht, W.: Nachrichtentechnik, Band II: Nachrichtenübertragung. Mannheim, Springer, 1982.
[40] Stratton, J.A.: Electromagnetic theory. New York, McGraw-Hill, 1941.
[41] Thaller, B.: Advanced visual quantum mechanics. Berlin, Springer, 2004.
[42] Thoma, P.; Weiland, T.: Wie real ist das Instantane Tunneln? Phys. Bl. 50 (1994), 313, 360, 361.
[43] Unger, H.-G.: Elektromagnetische Theorie für die Hochfrequenztechnik (Teil I). Heidelberg, Hüthig, 1981.
[44] Vakman, D.: Signals, oscillations and waves – a modern approach. Boston, Artech House, 1998.
[45] Zinke, O.; Brunswig, H.: Hochfrequenztechnik 1. Berlin, Springer, 1995.

Prof. Dr.-Ing. Klaus W. Kark
Hochschule für Technik, Wirtschaft und Sozialwesen Ravensburg-Weingarten
University of Applied Sciences
Doggenriedstraße 1
88250 Weingarten
Germany
Phone: +49 (751) 501-9591
Fax: +49 (751) 501-9876
E-Mail: kark@fh-weingarten.de
http://www.fh-weingarten.de/~kark

(Received on January 10, 2005)

Formelzeichen

$a_{1,2}$	waveguide width, m
b	waveguide height, m
c	$= c_0/\sqrt{\epsilon_r}$, velocity of Brillouin precursor, m/s
c_0	$= 2,99792458 \cdot 10^8$ m/s, speed of light in vacuum
d	attenuation per unit length, dB/m
d_x	time spread of input signal, s
$d_y(z)$	time spread of output signal, s
E	electric field, V/m
E	$= \hbar \omega$, photon energy, J
E_0	energy, J
E_1	first energy moment, Js
E_2	second energy moment, Js ²
f	frequency, Hz
f_c	cutoff frequency, Hz
f_e	electronic resonance frequency, Hz
f_0	carrier frequency, Hz
H	magnetic field, A/m
$H(\omega)$	magnitude spectrum
$\underline{H}(j\omega)$	complex transfer function
$h(t)$	impulse response
h	$\approx 6,6260688 \cdot 10^{-34}$ Js, Planck constant
\hbar	$= h/(2\pi) \approx 1,0545716 \cdot 10^{-34}$ Js
j	$= \sqrt{-1}$, imaginary unit
$\underline{k}(\omega)$	complex wave number, 1/m
l	length of photonic barrier, m
m	particle mass, kg
\vec{S}_R	time-averaged Poynting vector, W/m ²
t	time, s
$t_F(z)$	front delay, s
$t_{gr}(\omega)$	group delay, s
t_h	center delay, s
t_i	impulse delay, s
$t_p(z)$	peak delay, s
$t_{ph}(\omega)$	phase delay, s

t_x	gravity center of input signal, s
t_y	gravity center of output signal, s
$V(z)$	energy potential, J
$v_E(\omega)$	energy velocity, m/s
v_F	front velocity, m/s
$v_{gr}(\omega)$	group velocity, m/s
$\overline{v_{gr}}(z, \omega)$	spatially averaged group velocity, m/s
$\overline{v_p}(z)$	spatially averaged peak velocity, m/s
$v_{ph}(\omega)$	phase velocity, m/s
$\overline{v_{ph}}(z, \omega)$	spatially averaged phase velocity, m/s
w	spatial energy density, J/m ³
$\underline{X}(j\omega)$	input spectrum
$x(t)$	input signal
$\underline{Y}(j\omega)$	output spectrum
$y(t)$	output signal
$\alpha(\omega)$	attenuation constant, 1/m
$\overline{\alpha}$	mean attenuation, 1/m
$\beta(\omega)$	phase constant, 1/m
Δt	time step, s
δ	skin depth, m
$\delta(t)$	Dirac impulse, 1/s
$\epsilon(\omega)$	permittivity, As/(Vm)
$\epsilon_r(\omega)$	relative permittivity
ϵ_0	$= 1/(\mu_0 c_0^2) \approx 8,854 \cdot 10^{-12}$ As/(Vm), electric constant
κ	electric conductivity, S/m
λ	dielectric wavelength, m
λ_0	wavelength in vacuum, m
μ_0	$= 4\pi \cdot 10^{-7}$ Vs/(Am), magnetic constant
τ_x	energy center of input signal, s
$\tau_y(z)$	energy center of output signal, s
$\Phi(\omega)$	phase spectrum
Ψ	quantum mechanical wave function
ω	$= 2\pi f$ angular frequency (see f), 1/s

■ Buchbesprechung

Antennen und Strahlungsfelder

von Klaus Kark, 391 Seiten, 244 Abbildungen, 71 Tabellen, 65 Übungsaufgaben (durchgerechnet), Untertitel: Elektromagnetische Wellen auf Leitungen, im Freiraum und ihre Abstrahlung, Vieweg-Reihe „Studium Technik“, Wiesbaden 2004, ISBN 3-528-03961-2, Preis € 27,90.

Der Autor, seit 1993 Professor der Hochfrequenztechnik an der Fachhochschule Ravensburg-Weingarten, kann auf Erfahrungen aus Forschungsinstituten und der Industrie zurückgreifen; es richtet sich an FH- und TU-Ingenieure/Studenten („vorlesungsbegleitend“) sowie Physiker in der Praxis. Der Band gliedert sich in 17 Kapitel, einem Literatur- und Sachwortverzeichnis. Nach der Einleitung (Frequenzbereiche, Symbole, Antennenformen) folgen mathematische Grundlagen (Vektoranalysis und deren Integralsätze), wobei leider auf „grad, div, rot“ nicht verzichtet wird (redundant-doppelte Schreibweise zum Nabla-Operator: Kap. 8). Kap. 3 bringt Elektrodynamik (Maxwellgleichungen) samt Rand- und Stetigkeitsbedingungen, Relativitätssprinzip. Kap. 4: Ebene Wellen im freien Raum, auf Leitern und Supraleitern; Kap. 5: Kugelwellenausbreitung, Dopplereffekt bei Radar, wobei Kark einen „Fresnel'schen Mitführungseffekt“ (Zitat?) einführt; Welleneinfall auf (Mehr-)Schichten und Kanten (Beugung ohne Erwähnung der GTD). Kap. 6 widmet sich den Wellenleitern (koaxial, Hohl-, Streifenl.), wobei nicht vor „Orthogonalreihen-Entwicklung“ zurückgeschreckt wird; hier sollte man bei „Wellentypen“ (S. 143) bleiben und „moden“ erwähnen, „Oberwellen“ (S. 149, 343) statt „höhere Wellentypen“ sind hier falsch und gehören anderswo hin! Unnötige Anglizismen (wie Taperhohlleiter, statt verjüngter; Direktivität/Richtfaktor, S. 273) könnten vermieden werden. Mit Kap. 7

beginnt die Antennentechnik: ein isotroper Kugelstrahler (S. 152, 159, 256, 273) ist ein „weisser Schimmel“, wäre also besser durch „oder“ zu trennen. Bei der Antennenwirkfläche von Reflektoren (S. 167), d. h. deren „Flächenwirkungsgrad“ wäre eine Notiz hilfreich, daß man Solches heute durchaus (im %-Bereich genau) berechnen/integrieren kann. Kap. 8 bringt – gut gegliedert – Grundbegriffe von Strahlungsfeldern: wäre zu ergänzen, daß bei Phasenmessungen der Fernfeldabstand (S. 189) das Vierfache des normalen (Leistungs-)Abstandes sein kann. Kap. 9 überstreicht Elementardipole und Rahmenantennen samt Erwähnung deren „Grenzzadius“ und „Abschnürradius“ der Kugelwellen.

Kap. 10 bezieht sich auf Lineare (Stab-)Antennen (endlicher Dicke), wobei u. a. auf numerische Lösungen von (komplexen) Intergralgleichungen hingewiesen wird – recht erstaunlich (!) für eine FH-Vorlesung...Der „Verkürzungsfaktor“ wird sehr anschaulich erklärt. In Kap. 11 folgen die unverkoppelten und verkoppelten (auch „verdünnten“) Gruppenantennen (phased arrays). Bei Erwähnung des „multiplikativen Gesetzes“ vermißt man das Nennen des Überlagerungsprinzips (der EM-Wellen) Kap. 12 geht auf die Diagramm- und Impedanz-Variante breitbandiger Antennen ein, wobei log-periodische Typen Rückwärtswellen anregen. Kap. 13, 14 behandeln Hohlleiter- und Hornstrahler; warum kann eine „Designgleichung“ (S. 342, 353) hier nicht schlicht Entwurfsleichung sein? Kap. 15, 16 beschäftigen sich mit Linsen- und Reflektorantennen. Das Buch schließt mit Schlitz- und Plättchen-Antennen (patch), Kap. 17. Im Sachwortverzeichnis ist Einiges ergänzbar. Insgesamt gesehen stellt der Band ein sehr modernes und nützliches Buch für die genannten Zielgruppen dar (Übungsaufgaben!) und ist sogar als Nachschlagewerk benutzbar. Es ist ihm in Fachkreisen weite Verbreitung zu wünschen.

Rudolf Wohlleben, Bonn/Bad Kreuznach